Proceedings of ASME Turbo Expo 2008: Power for Land, Sea and Air
GT2008
June 9-13, 2008, Berlin, Germany

GT2008-51514

DESIGN, DEVELOPMENT AND TEST OF A 30 KW OIL-FREE, TURBOALTERNATOR

Hooshang Heshmat, Ph.D. (ASME/STLE Fellow)
hheshmat@miti.cc
Mohawk Innovative Technology Inc.
Albany, NY 12205

James F. Walton II (ASME Fellow)
jwalton@miti.cc
Mohawk Innovative Technology Inc.
Albany, NY 12205

Michael J. Tomaszewski
mtomaszewski@miti.cc
Mohawk Innovative Technology Inc.
Albany, NY 12205

ABSTRACT

This paper describes the design procedures and testing program used in the development of a 30 kW single shaft permanent magnet turboalternator with compliant foil bearing supports. The development program included design tradeoff studies assessing generator rotor and bearing configurations, design of the turbine, and packaging of the entire system. This paper also describes the test program to assess dynamics, thermal management of the system and testing to assess power output. Test results achieved with the prototype system operating to full speed and under power generating mode will be presented. A comparison between predicted and measured electrical output will also be presented up to a power generating level of 25 kWe at approximately 55,000 rpm. The excellent correlation between design and test provides the basis for scale up to larger power levels. This program demonstrates the successful integration of oil-free foil bearings, 4-pole composite wound permanent magnet alternator, thermal management capabilities and an axial flow turbine

INTRODUCTION

As demands for renewable energy production rise and demand for low environmental impact, oil-free machines with high operating speeds that directly drive alternators are becoming increasingly appealing as replacements for existing technologies. The tightly integrated and directly connected machines offer higher efficiencies, are generally smaller and quieter, and require less maintenance when using oil-free compliant foil bearings. The successful implementation of an oil-free, turboalternator relies essentially on the availability of five major elements: (1) an efficient, high-speed alternator/generator; (2) the necessary complimentary power electronics; (3) state-of-the-art aerodynamics; (4) reliable and low power loss bearings; and (5) the supporting systems such as coolers, filters, etc. All of these needs can be met by today's technology. State-of-the-art, high-speed, permanent magnet alternators are available in power ranges from a few to several hundred kilowatts, with high operating speeds [1-4]; state of the art turbines provide efficiencies above 75%; and advanced oil-free foil bearing technologies allow operation under large loads and even above the first bending critical speed [5-11]. These technologies have resulted in numerous microturbines being developed and in service data being evaluated such as shown in [12]

Given the speeds ranges and environment of these new machines, the performance, reliability and durability requirements placed on the bearings are severe. Conventional rolling element bearings are subjected to extreme conditions due to the speed and load capacity required. Additionally, an external lubrication, and filtration systems are required for the bearings. The alternative of oil-lubricated hydrodynamic bearings is not much more appealing. Again, a lubrication system is required, and at the high speeds envisioned for these machines, there will be significant bearing power loss. The requirement for a lubrication system for either of these alternatives also brings with it the requirements for a sealing system with its inherent losses, leakage, as well as oil separators.

With the current emphasis on the environment and the increasing costs of fuel, there is a desire to increase the use of renewable energy. One solution is a renewable energy, low-temperature, turbine driven generator system shown schematically in Figure 1. This closed loop Rankine cycle feeds high kinetic energy vapor to an expander turbine, driving the generator thereby decreasing the vapor temperature and pressure. The cold gas is then condensed to liquid and pumped to the evaporator where either process waste heat or heat from a variety of the heat sources causes the refrigerant to boil and vaporize. Preliminary analysis has determined that approximately 1-2 Million BTU/hour are readily available from industrial or utility cooling ponds. Alternatively waste

heat from industrial processes could be used to power the system. By using waste heat in its many forms this renewable energy power generating system will have no environmental impact. Additionally since there is no fuel cost, it minimizes end user operating costs and the generated power would increase utility efficiency or reduce electricity costs for a plant using such a system [13-18]. While many studies have been completed over the years and micro gas turbine are being manufactured today, the Oil-Free renewable energy powered turboalternator discussed herein addresses the integration of components into a single shaft so that the system will result in a compact, efficient, low-cost, environmentally friendly system for electricity generation. It offers utility, self-generators and industrial operators an attractive resource to use low-grade waste heat for power generation.

In this paper MiTi® will present preliminary proof of concept data from a prototype, integrated single-shaft turboalternator demonstrator system that was built and tested with air. Ultimately, this system is planned to operate with appropriately selected refrigerant, which will depend upon the operating temperature of the available waste heat. When designing the system to operate with a selected refrigerant, the key components will need to be reviewed to ensure their ability to operate with the selected refrigerant. For example because the system is to be hermetically sealed, the bearings must be able to operate with either gas or two-phase flow, which is known to cause rotordynamic stability issues if not properly accounted for. Besides dynamic stability, materials compatibility with the refrigerant must be assured. With the sub-scale system successfully demonstrated, systems capable of producing 200+ kW to megawatt sizes appear feasible.

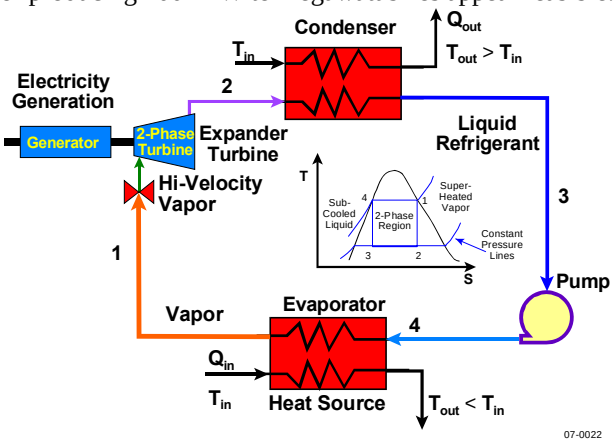

Figure 1 Renewable energy system schematic using high mach velocity gas.

TURBOGENERATOR DESCRIPTION

The turbogenerator demonstrator system that has been designed, fabricated and assembled is shown in Figure 2 through Figure 4. Included in the system design were the controls and safety interlocks to control shaft speed, turbine inlet gas pressure, prevent turbine overspeed whether power is being extracted or not and provide an emergency stop. During preliminary testing it has been shown that turbine exhaust gas can be used to cool the generator stator and rotor elements as evidenced by the stable temperatures of the stator and bearings. The ability to use exhaust gas for system thermal management is a key benefit to the overall system since elimination of an external cooling source will help reduce the cost of manufacturing.

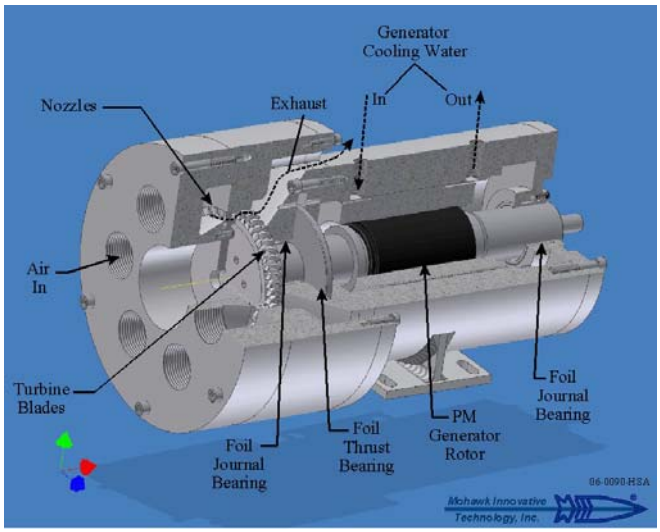

Figure 2 Cross section drawing of turboalternator

Figure 3 Turbogenerator component assembly

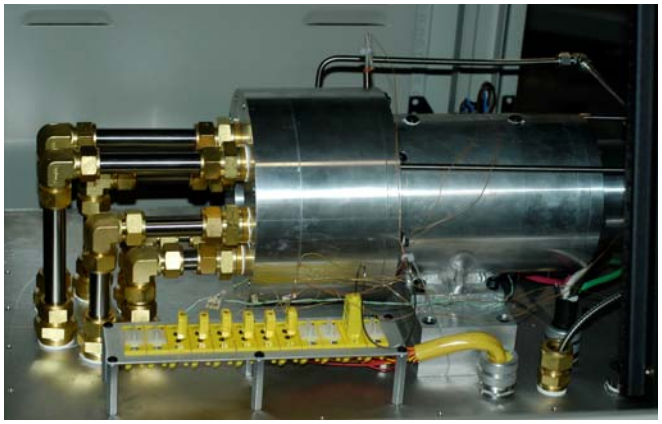

Figure 4 Assembled turbogenerator in cabinet

The high-speed, permanent magnetic alternator is located between the two journal bearings. Provision was included to provide for liquid cooling of the stator if needed. The double acting foil thrust bearing is located at one end of the rotor

adjacent to the turbine end journal bearing. The overall rotor length including the turbine is 293 mm. The overall mass of this multi-component rotor system with turbine wheel is approximately 3.4 kg. The journal bearings, sized to accommodate the corresponding static loads, are 30 mm long by 36 mm in diameter. The thrust bearing has a 36.5 mm ID and a 96 mm OD. These bearing sizes are the result of a number of component and system design iterations to ensure stable rotor-bearing system operation and long bearing life under the expected conditions of operation for this turbine. Additional concerns, including thermal issues, manufacturability and system reliability were also considered during these iterations. The compactness and power density of the system is evidenced by the maximum outer diameter and length of 203 mm and 323 mm respectively, excluding the external plumbing.

ROTORDYNAMICS

A key element in the design of any high-speed machine is the rotor system design and dynamic analysis. For this project, a finite-element model of the rotor was used (see Figure 5). This model includes four different shaft materials to model the main shaft, turbine wheel, and composite wound permanent magnet (PM) alternator sleeve construction. The model of the PM sleeve section assumed a material density of 7086 kg/m^3 based on the combined magnet and composite materials. Similarly, the material modulus of E=2.1E+7 and G=1.5E+7 kPa was modeled as a combination of both the composite wrap and magnet materials. Table 1 and Table 2 present the foil bearing dynamics coefficients used in the rotor analysis.

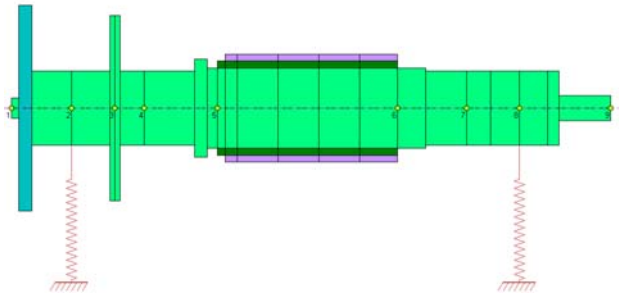

Figure 5 Finite element rotor-bearing system model

Table 1 Foil bearing dynamic stiffness coefficients (N/m)

Speed	Kxx	Kxy	Kyx	Kyy
20000	977381	-106652	-898049	2120607
30000	976155.1	-107528	-926069	2105196
45000	1044104	30296.88	-874932	2015181
60000	1102596	131344.9	-827823	2037422

Table 2 Foil bearing damping coefficients (N-s/m)

Speed	Bxx	Bxy	Byx	Byy
20000	403	0	0	403
60000	403	0	0	403

It is assumed for preliminary analysis that the minimum predicted value of damping is used at all speeds to ensure adequate stability margin over all speeds

Based on the finite element rotor model and foil bearing coefficients presented, rotor bearing system analysis was conducted. Figure 6 through Figure 8 present the first three natural frequencies when operating at 60,000 rpm.

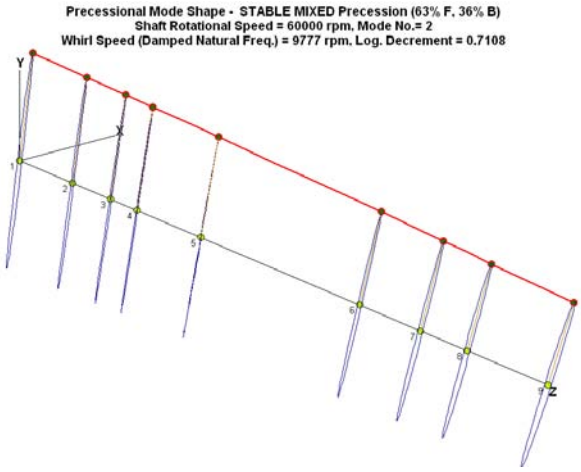

Figure 6 First rigid body natural frequency for 60,000 rpm operating speed

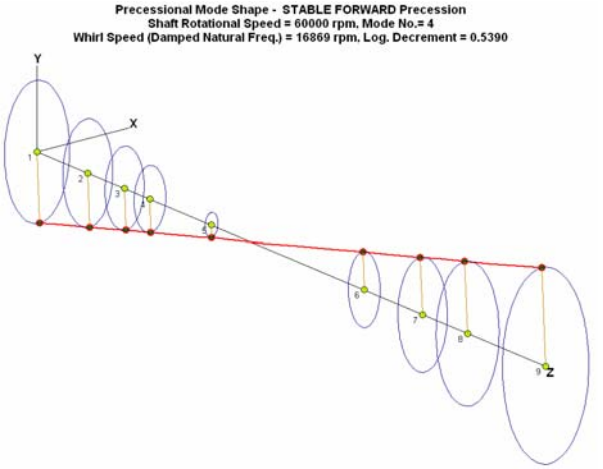

Figure 7 Second rigid body natural frequency for 60,000 rpm operating speed

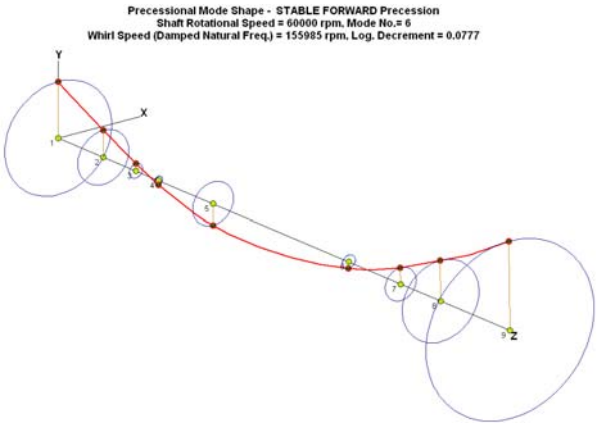

Figure 8 Third rigid body natural frequency for 60,000 rpm operating speed

Given that the maximum design operating speed is 60,000 rpm, the placement of the natural frequencies and the high logarithmic decrements for the lower modes, smooth stable operation was expected. For example the first critical speeds are predicted to occur at approximately 9700, 15,600 and 169,000 rpm. When operating at 60,000 rpm the first three natural frequencies occur at approximately 9800, 16,900 and 156,000 rpm for the low damping level used.

TEST SETUP AND CHECKOUT TESTS

This section of the paper describes the test setups used for rotor-bearing system dynamic and preliminary turboalternator performance testing. A total of 10 temperatures, 4 pressures, 1 displacement and one speed signal were included in the instrumentation as shown in Figure 9. The completed assembly is shown in Figure 4.

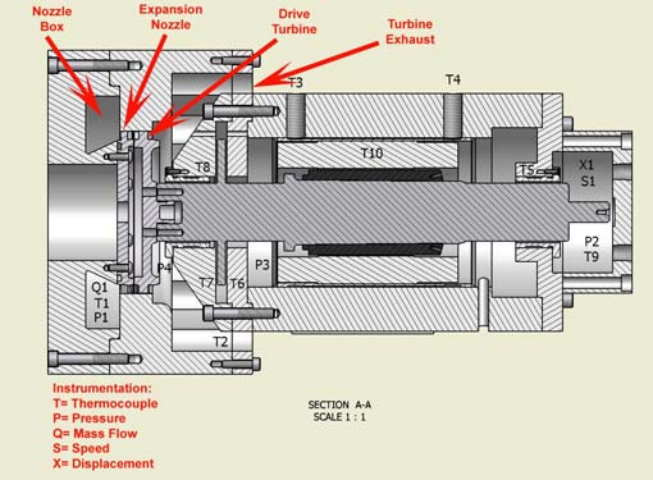

Figure 9 Turboalternator cross section showing instrumentation

Preliminary testing was completed to verify operation and stable thermal and rotordynamic performance of the turboalternator to full speed under no load conditions. Figure 10 shows that full speed was achieved, maximum vibrations were less than 22.9 micron and the first two critical speeds occurred at approximately 9,600 and 12,600 rpm. If damping levels are increased to 1200 n-s/m, a factor of 3 over the initial predictions the second mode drops to 14,500 rpm. Given the broad peaks seen in rotor response of Figure 10, this appears a valid assumption. Figure 11 shows stable thermal operation of the bearings and generator stator as for the given turbine inlet and exhaust temperatures. A maximum thrust foil bearing temperature of 75°C was observed for the loaded side bearing, nearest the turbine. The corresponding turbine side journal foil bearing reached a maximum temperature of 64°C. The generator stator and thrust bearing maximum temperatures did not exceed 35°C. Finally the free end journal bearing temperature was approximately 12°C.

TESTING

Once both rotor-bearing system dynamic and system thermal stability were demonstrated, testing under electrical generator loads was initiated. Figure 12 shows results of the initial testing of the assembled system under 50 % electrical load. For this first series of tests to 60,000 rpm total output power was on the order of 16 kW. Figure 13 shows measured system data under the 50% load testing. During this testing inlet turbine air temperature was approximately 7°C with resultant outlet air temperature at –40°C. Figure 14 shows that the system bearing and stator temperatures remained well controlled even with not external cooling applied.

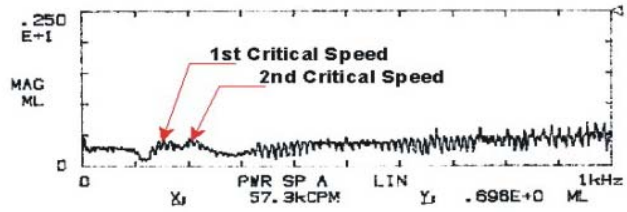

Figure 10 Shaft synchronous vibration during operation to full speed demonstrating

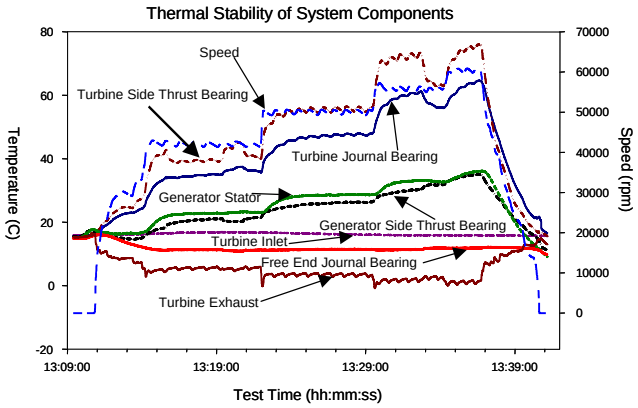

Figure 11. No load system thermal characteristics

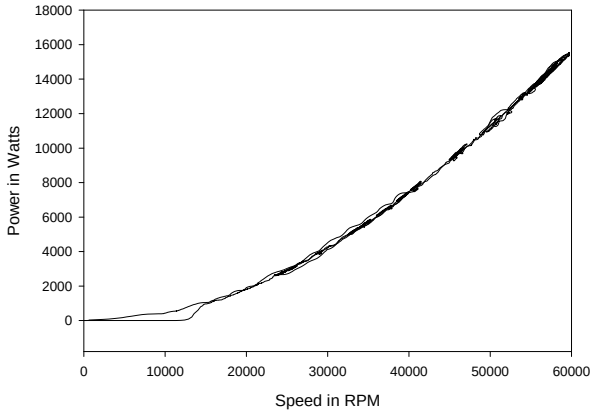

Figure 12. Measured output power as a function of speed

Following the 50% load testing, the system was configured for 100% load testing. Under these tests speed was limited to between 54,000 to 59,000 rpm due to available airflow from in-house facilities. As seen in Figure 15, testing to just below 60,000 rpm was achieved with turbine inlet temperature of approximately 16°C. Under full load, the turbine exhaust temperature dropped to approximately -57°C. Figure 15 also compares predicted and measured power output for the system showing excellent correlation. Figure 16 shows the thermal characteristics under 100% load. Bearing temperatures all

remain well below the stator temperature, which remains below 40C, with only exhaust gas cooing employed. Figure 17 and Figure 18 compare predicted performance of the permanent magnet alternator performance as a function of speed to measured output. As seen, with the exception of very low operating speeds, there is excellent correlation between the measured and predicted voltage, current and power for the given 9.3 ohm resistive load.

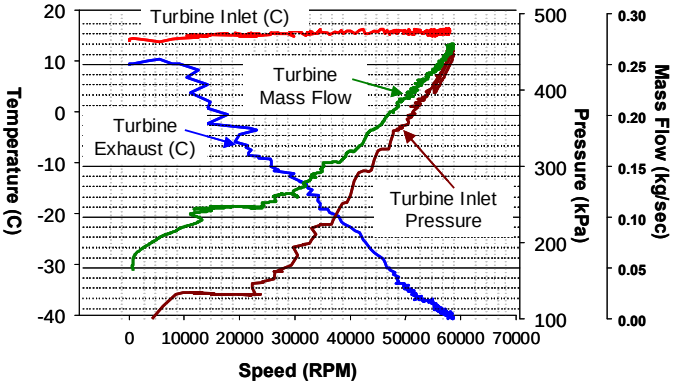

Figure 13 Measured system parameters during 50% load testing

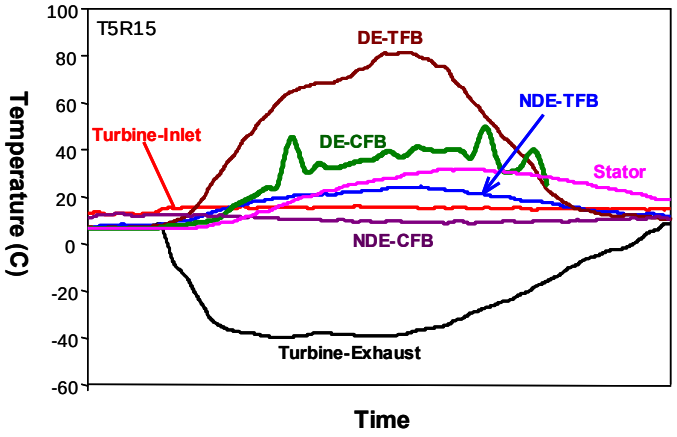

Figure 14 Component Temperatures during 50% load testing

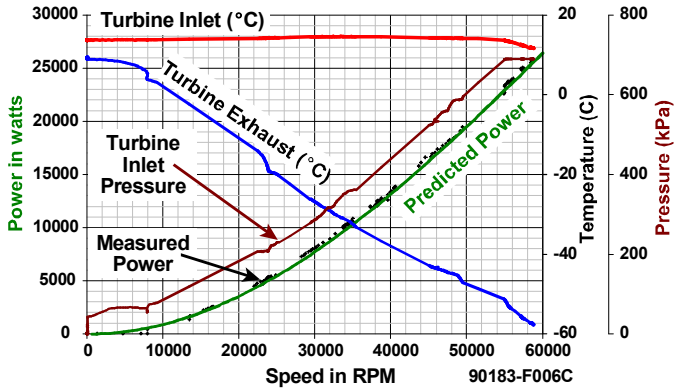

Figure 15 System measured performance at 100% load

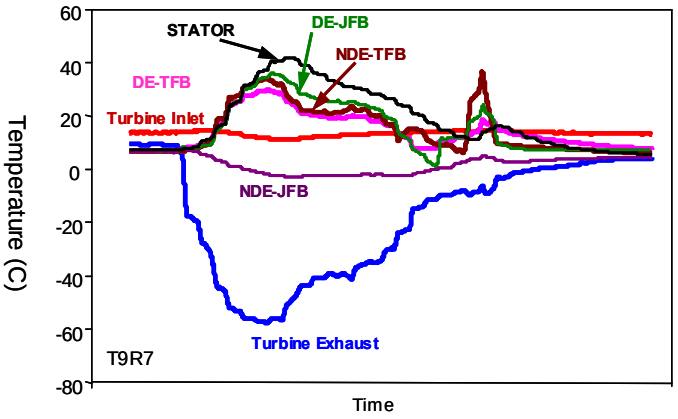

Figure 16 Thermal characteristics under 100% load

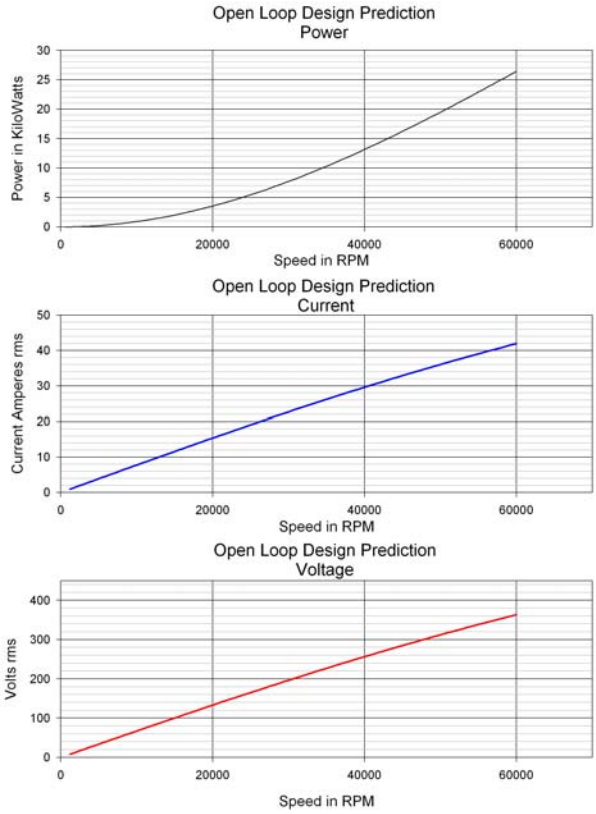

Figure 17 Open loop PM alternator output prediction versus speed for 9.3 ohm resistive load

SUMMARY AND CONCLUSIONS

In summary, a 30 kW directly driven turboalternator has been designed, developed and successfully tested. This effort validated the design process employed as evidenced by the observed rotor-bearing system dynamic stability, stable bearing and stator temperatures and the measured electrical output. During testing dynamic and thermal stability were demonstrated. The extremely small size and resulting high power density did not pose any difficulty in the system thermal stability as evidenced by the minimal temperature rise in the bearings and the stator. Additionally, differences

between predicted and measured critical speeds were minimal even when the lowest high-speed damping levels were assumed for all operating speeds. Consequently, the feasibility of using the tested design to develop a compact, high performance, oil-free direct drive turboalternator system as an alternative to existing microturbine designs that use coupled shafting and/or more than two journal bearings has been demonstrated. Additional testing is planned to more completely characterize the system performance, identify an appropriate refrigerant and demonstrate operation, life and durability with the selected refrigerant.

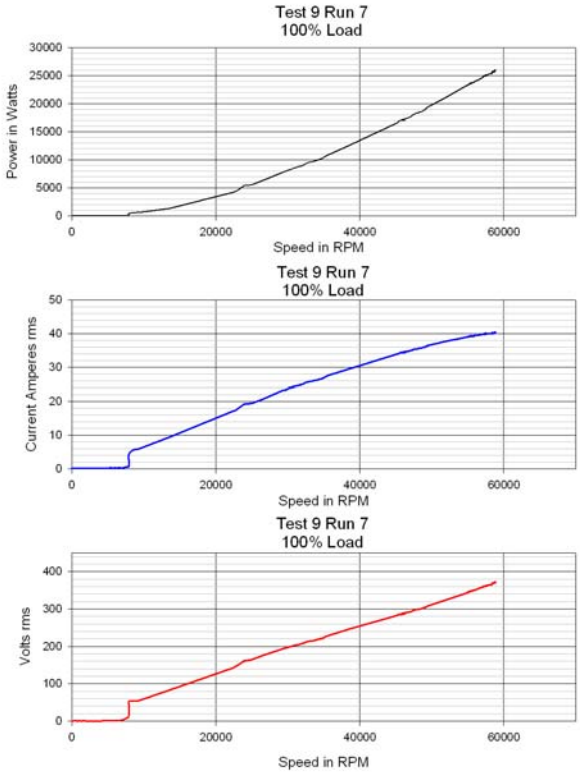

Figure 18 Measured turboalternator electrical output

ACKNOWLEDGMENTS

The authors would like to thank Mohawk Innovative Technology, Inc. and Today's Technology for supporting this effort.

REFERENCES

[1] U.S. Department of Energy, 2000 "High-Speed Permanent Magnet Motor Development For Advanced Cooling Technology," DOE/GO-102000-0844 Order# I-OT-741

[2] Swanson, E.E., Heshmat, H., & Shin, J.S., 2002, "The Role Of High Performance Foil Bearings In An Advanced, Oil-Free, Integral Permanent Magnet Motor Driven, High-Speed Turbo-Compressor Operating Above The First Bending Critical Speed" ASME Paper GT-2002-30579

[3] Walton, J.F., II, Tomaszewski, M.J. and Heshmat, H., 2003 "The Role of High Performance Foil Bearings in Advanced, Oil-Free, High-Speed Motor Driven Compressors." ASME Paper Fuel Cell 2003-1747, *1st International Conference on Fuel Cell Science, Engineering and Technology*, Rochester, New York.

[4] Walton, J.F., Tomaszewski, M.J., Heshmat, C.A., Heshmat, H., 2006, "On The Development Of An Oil-Free Electric Turbocharger For Fuel Cells," ASME Paper GT2006-90796.

[5] Suriano, F. J., Dayton, R. D., & Woessner, F. G., 1983, "Test Experience with Turbine-End Foil Bearing Equipped Gas Turbine Engines." ASME Paper No. 83-GT-73.

[6] Heshmat, H. and Hermel, P., 1992, "Compliant Foil Bearing Technology and their Application to High-speed Turbomachinery." *19th Leeds-Lyon Symposium on Thin Film in Tribology - From Micro Meters to Nano Meters, Leeds*, UK. D. Dowsen, et. al., eds., Elsiver, pp. 559-575.

[7] Heshmat, H., 1994, "Advancement in the Performance of Aerodynamic Foil Journal Bearings- High Speed and Load Capacity", ASME J. of Tribol., 116, pp 287-95.

[8] Heshmat, H., 2000, "Operation of Foil Bearings Beyond the Bending Critical Mode." ASME J. of Tribol., 122(2), pp. 192-198.

[9] San Andrés, L., Rubio, D., and Kim, T. H., 2006, "Rotordynamic Performance of a Rotor Supported on Bump Type Foil Gas Bearings: Experiments and Predictions," ASME Paper GT2006-91238.

[10] Salehi, M., Heshmat, H. and Walton, J.F., 2003, "On the Frictional Damping Characterization of Compliant Bump Foils." ASME J. of Tribol., 125 (4), pp. 804-813.

[11] Heshmat, H., 2005, "Major Breakthrough in Load Capacity, Speed and Operating Temperature of Foil Thrust Bearings." ASME Paper WTC2005-63712.

[12] Liekens, J., Van Bael, J., Desmedt, J., Robeyn, N., Jannis, P., 2005, "Results From The Research On Microturbine-Chp-Applications In Flanders," ASME Paper GT2005-68110

[13] Obert, E.F. and Gagglioli, R.A., 1963, *Thermodynamics*, 2nd Edition, McGraw-Hill Book Company, New York

[14] Kreith, W., and West, R.E., 1997, CRC Handbook of Energy Efficiency, CRC Press, Boca Raton, FL., pp. 671-687

[15] Bogo, J., 2008, "Geothermal Power in Alaska Holds Hidden Model for Clean Energy," Popular Mechanics, February 2008

[16] Sadeghi, E., Khaledi, H., and Ghofrani, M. B., 2006, "Thermodynamic Analysis Of Different Configurations For Microturbine Cycles In Simple And Cogeneration Systems," ASME Paper GT2006-90237

[17] PureComfort TM Cooling, Heating & Power Solutions.; UTCPower.http://www.utcpower.com/fs/com/bin/fs_com_Page/0,5433,03200,00.html

[18] D. Dewis Absorption Chiller Integrated System Development http://eere.energy.gov/de/pdfs/conf-04_micro_appswkshp/dewis.pdf